Surface Structure Determination of an Oxide Film Grown on a Foreign Substrate: Fe_3O_4 Multilayer on Pt(111) Identified by Low Energy Electron Diffraction

W. Weiss, A. Barbieri, M. A. Van Hove, and G. A. Somorjai

Materials Sciences Division, Lawrence Berkeley Laboratory, University of California, and Department of Chemistry, University of California, Berkeley, California 94720

(Received 24 May 1993)

For the first time a detailed surface structure determination is reported for an oxide film grown on a foreign metal substrate. Well-ordered iron oxide films were grown onto Pt(111) substrates and were identified by a dynamical low energy electron diffraction analysis to be magnetite, Fe_3O_4. They form an unreconstructed polar (111) surface termination that exposes $\frac{1}{4}$ monolayer of Fe ions over a distorted hexagonal close-packed oxygen layer and minimizes the number of dangling bonds. The surface also exhibits large relaxations that may be driven by electrostatic forces.

PACS numbers: 61.14.Hg, 68.35.Bs

There is increasing interest in the surface properties of metal oxides because of their important technological applications as catalyst materials and corrosion resistant coatings. Furthermore, the magnetic properties of the different oxides of iron are utilized for the development of high density magnetic recording media. The knowledge of the structure and energetics of oxide surfaces is essential for an understanding of their physical and chemical properties. A number of theoretical total energy calculations predict large surface relaxations away from the bulk terminated structures, especially for the polar surfaces, leading to substantial reductions of their surface free energy [1,2]. Very few experimental studies on the surface crystallography of metal oxides have been carried out so far, and a relatively small number of oxide surfaces, primarily of the NaCl(100) type, have been analyzed by low energy electron diffraction (LEED) and other techniques [3,4]. This is mainly due to the difficult preparation of clean and ordered surfaces of these materials, since single crystals of bulk oxides often contain impurities that can segregate to the surface in ultrahigh vacuum. Furthermore, oxides are usually electrical insulators; this causes electrostatic charging problems when using electron spectroscopy techniques.

One way to overcome these problems is to prepare thin oxide films by oxidizing metal single crystal surfaces, which was done for example on Fe [5], Ni [6], Co [7], and Mo [8] single crystals. The oxidation of an alloy $Ni_{60}Fe_{40}(100)$ surface led to the formation of an ordered Fe_3O_4 film [9], and ordered Al_2O_3 films were prepared by oxidizing a NiAl(110) surface [10]. However, it is difficult to control the composition and thickness of oxide films prepared in this way, because the oxygen from the surface oxide may diffuse into the metal substrate, thereby changing these parameters. We have chosen a different approach in preparing ordered oxide surfaces. We deposit a monolayer (ML) of a metal, in this case iron, on an ordered crystal face of another metal, in this case Pt(111). Then we oxidize the deposited metal and heat to order the oxide monolayer. This process is repeated to grow a second layer onto the first monolayer, and so on. In this way, while the platinum substrate does not oxidize, the thickness of the iron oxide layers can be controlled, as well as, to a certain extent, their composition. Iron oxide forms well-ordered films when prepared in this way. This Letter reports the first structural analysis of an epitaxially grown metal oxide film by LEED, demonstrating that surface crystallography of even complex metal oxide surfaces prepared in such a way is well within reach of LEED analysis. A more detailed account will be published elsewhere [11].

The platinum single crystal was mounted in an ultrahigh vacuum chamber equipped with four-grid LEED optics, a cylindrical mirror analyzer Auger spectrometer, and a mass spectrometer. The base pressure was 4×10^{-10} mbar. The sample could be heated by electron bombardment from the back and cooled by a liquid nitrogen reservoir. The temperature was measured with a chromel-alumel thermocouple spotwelded to the back of the crystal. The Pt(111) surface was prepared by repeated cycles of sputtering with 1 keV Ar^+ ions and subsequent annealing to $T=1500$ K in 2×10^{-7} mbar oxygen. A final flash to that temperature without oxygen resulted in a clean surface as detected by Auger electron spectroscopy (AES) and in a sharp (1×1) LEED pattern. Iron was evaporated from a 99.999% pure iron wire wrapped around a resistively heated tungsten wire with deposition rates between 1 and 5 Å/min. After we deposited 1 ML of iron onto the clean Pt(111) surface, we heated for 2 min in 10^{-6} mbar oxygen to $T=1000$ K and slowly cooled down to room temperature afterwards. This produced a well-ordered oxide monolayer as detected by LEED. Then we repeated this procedure to grow the oxide film layer by layer. No contaminations were detected by AES in these films; their thickness was determined by the attenuation of the platinum substrate Auger signal as described earlier [12].

Because of the lattice mismatch, a 1 ML thick iron oxide film forms hexagonal coincidence structure with respect to the platinum substrate, which has a lateral lattice constant of 3.2 Å on its surface as obtained from the LEED pattern [12]. Between 1 and 2 ML coverage a

0031-9007/93/71(12)/1848(4)$06.00

new hexagonal LEED pattern appears with spots corresponding to a lateral lattice constant of 3.0 Å that we shall call integer order spots and new half order spots. The spot positions indicate a lateral contraction of the second oxide layer with respect to the first layer underneath. This LEED pattern, from now on referred to as a (2×2) pattern, remains unchanged up to 10 ML film thickness, the thickest film we prepared The intensities of twelve inequivalent beams of an 8 ML thick film were recorded under normal incidence at 100 K by use of a video camera connected to a computer onto which the data could be stored. Intensity-voltage (*I-V*) curves of symmetrically equivalent beams were averaged before being analyzed. It is important to mention that we were able to reproduce these data by using a very different approach. In a separate experiment we prepared the (111) surface of an α-Fe_2O_3 single crystal doped with germanium by sputtering with 1 keV Ar^+ ions and prolonged annealing to $T=1000$ K. This preparation resulted in the same (2×2) LEED pattern with intensity-voltage curves identical to those obtained from the epitaxial films, indicating that the surface region of the single crystal was reduced to Fe_3O_4 and had the same structure as the epitaxially grown films [11].

Iron forms a number of oxides with different stability ranges [13]. FeO (wustite) crystallizes in the cubic sodium chloride structure, Fe_3O_4 (magnetite) in the cubic inverse spinel structure, and α-Fe_2O_3 (hematite) in the rhombohedral crystal structure of corundum. The metastable γ-Fe_2O_3 has a cubic spinel structure very similar to Fe_3O_4. All these oxides can transform into each other depending on the ambient conditions (temperature, oxygen pressure) and it is not *a priori* obvious which structure the film grown under our conditions should form. Along the [111] direction these oxides can be viewed to a very good approximation as a stacking of close-packed oxygen layers: cubic *ABCABC* stacking in the case of FeO and Fe_3O_4 and hexagonal *ABAB* stacking in the case of α-Fe_2O_3. Because of the different positions of the iron atoms between the oxygen layers a bulk (111) surface termination or a relaxed version thereof would give rise to different LEED patterns in the three cases. With respect to a two-dimensional cell on the hexagonal (111) surface with dimensions of 3.04 Å for FeO, 2.97 Å for Fe_3O_4, and 2.90 Å for α-Fe_2O_3 [14] a (1×1), a (2×2), and a $(\sqrt{3}\times\sqrt{3})R30°$ LEED pattern would be obtained, respectively. Since we observe a (2×2) LEED pattern we rule out an α-Fe_2O_3 overlayer, while several reconstructed forms of FeO(111) were excluded by explicit *I-V* curve analysis as well as by the stoichiometry obtained from the AES measurements, which was close to that of Fe_3O_4 [11].

The structure of Fe_3O_4 contains iron atoms that are octahedrally and tetrahedrally coordinated to oxygen atoms. Along [111] they form an alternating sequence of two distinct layers separated by the oxygen layers, the first containing only octahedral and the second both octahedral and tetrahedral atoms. This can be seen in Fig. 1(a) which shows a side view of the final structure determined by our LEED analysis. Computationally, the short distances (0.6 and 1.20 Å) between the (111) planes can cause convergence problems in a LEED calculation. This problem was solved by treating the structure as a sequence of two different composite layers whose diffraction matrices were computed exactly by the Beeby inversion scheme. The renormalized forward scattering method could then be used in the usual way to account for multiple scattering between the layers [15]. We used seven phase shifts generated for Fe^{2+} and O^{2-} ions forming the FeO structure [11], but checked that the results depend only very weakly on the oxidation state of the atoms. For temperature modeling we used $\theta_D=500$ K, a value comparable to the Debye temperature of other metal oxides [16], and again checked that the structural determination is quite insensitive to this nonstructural parameter. The imaginary part of the inner potential was

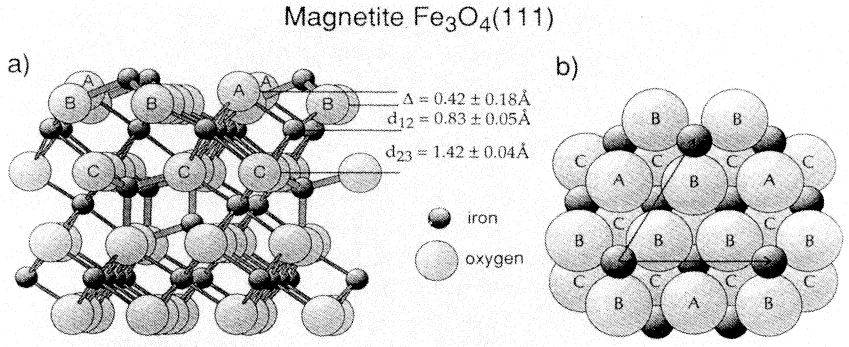

FIG. 1. (a) Perspective side view of the Fe_3O_4(111) surface structure (surface is on top). Relaxed layer spacings in the surface region are indicated. The corresponding bulk values are $\Delta=-0.04$ Å, $d_{12}=d_{23}=1.19$ Å. Bonds formed by tetrahedral and octahedral iron atoms are drawn thick and thin, respectively. Tetrahedral sites are occupied by Fe^{3+} ions; octahedral sites are occupied randomly by 50% Fe^{2+} and 50% Fe^{3+} ions. The ionic sizes are reduced by a factor of 0.5. (b) Top view onto the Fe_3O_4(111) surface with the full ionic sizes. The lattice vectors of the (2×2) unit cell are also indicated.

set to 4 eV, while the real part was determined in the course of the fitting procedure. The Pendry R factor R_P was used to quantify the theory-experiment fit.

The (111) surface of Fe_3O_4 has six possible unreconstructed surface terminations and the number of possible different surface structures rapidly increases if we include models with vacancies, adatoms, or other reconstructions. Our strategy to limit the time of search for the best structure was the following: (a) We only considered terminations and vacancy models having reasonable bond distances and the $p3m1$ symmetry of the ideally terminated (111) cut of the spinel structure; (b) we used automated search codes [17] based on the tensor LEED approximation [18] to analyze these different structures and to determine quickly the best relaxed surface structure in each case. To speed up the analysis and to enhance reliability, a first selection giving the best I-V curve fit was done by analyzing the six strongest beams ([0,1],[1,0], [1,1],[1/2,0],[0,1/2],[1/2,1/2]) in the energy range 50 -250 eV. We allowed relaxations compatible with $p3m1$ symmetry for the top 10–12 atoms (depending on the termination) in the (2×2) unit cell, and assumed an "ideal spinel" structure [14]. At this stage we also investigated the possibility of two different coexisting surface terminations separated by steps one oxygen interlayer distance high. This was done by relaxing simultaneously the coordinates of the two terminations, which were mixed incoherently: This did not improve the R factor significantly. Our analysis suggests that if different terminations indeed coexist, one of them is covering less than 30% of the surface. The final refinements on the best structure were done using twelve beams in the range 90–300 eV, giving a cumulative energy range of 2400 eV. Here the "ideal spinel" approximation [14] was lifted and relaxations compatible with the $p3m1$ symmetry were allowed for atoms whose distance from the surface was less than 6 Å. A selection of representative I-V curves corresponding to the best fit structure is shown in Fig. 2.

Our preferred structure is shown in Fig. 1 and corresponds to an overall R factor of $R_p=0.46$. Considering the complexity of the structure and the fact that we are analyzing an epitaxially grown film, this value is reasonable. We are not aware of a LEED crystallography study of a compound structure of comparable complexity. Perhaps the most similar system in this respect is the $SrTiO_3(100)$ surface, for which an R factor of $R_p=0.53$ was reported [3]. Our surface structure corresponds to a strongly relaxed bulk (111) termination in which the layer containing two tetrahedral and one octahedral iron atoms is cut so that one single tetrahedral iron atom per (2×2) unit cell is left at the surface and is now coordinated to three oxygen atoms underneath. It is intriguing that among all possible terminations of the $Fe_3O_4(111)$ surface this is the one with the minimum number of dangling bonds. A schematic top view of the surface is shown in Fig. 1(b). The main feature of the surface relaxation is the $\Delta=0.42\pm0.18$ Å upward displacement of the surface oxygen atom labeled "A" (which is not bonded to a surface iron) with respect to the oxygen atoms labeled "B" (which are bonded to a surface iron). In the bulk this displacement is much smaller (0.04 Å) and in the opposite direction. It reduces the height difference between the surface iron atom and the displaced oxygen atom "A" from 0.65 Å to 0.40 ± 0.05 Å, which presumably decreases the electrostatic surface dipole layer of the unreconstructed termination. This suggests that the large relaxations are driven by ionic forces which tend to decrease the electrostatic surface energy of the unreconstructed termination. Another feature of the surface relaxation is the change in spacings between the second iron layer and the plane formed by the equivalent "B" oxygen atoms above and the equivalent oxygen atoms labeled "C" below it. The first spacing d_{12} decreases by 30% from 1.19 Å to 0.83 ± 0.05 Å and the second spacing d_{23} increases by 20% from 1.19 Å to 1.42 ± 0.04 Å. In terms of bond lengths the bulk Fe_3O_4 structure has two types of Fe-O bonds: short (1.88 Å) and long (2.07 Å). Tetrahedral iron atoms have four short bonds and octahedral iron atoms have six long bonds, whereas each oxygen atom has one short and three long bonds. Our favored unreconstructed termination leaves each surface atom with one dangling bond; long in the case of the three "B" oxygen atoms, short in the case of the "A" oxygen and the surface iron. The structural relaxations at the surface shorten the remaining bonds of the "B" oxygen atoms, which now form two short bonds (1.87 Å) to the second layer iron atoms and one longer bond (1.98 Å) to the surface iron atom, the latter now forming three such 1.98 Å bonds to the "B" oxygen atoms. The "A" oxygen atoms

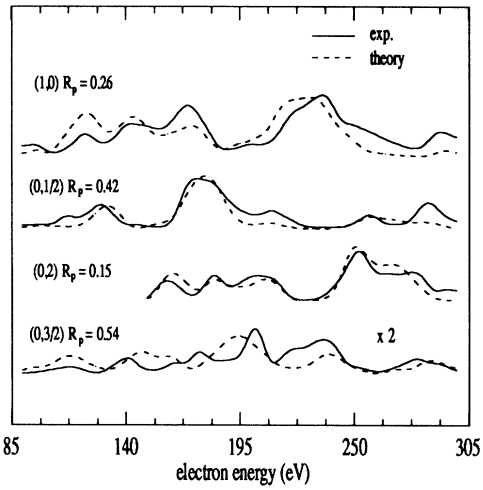

FIG. 2. Comparison between the experimental (solid curves) and theoretical (dashed curves) intensity-voltage spectra from a representative selection of beams. The R_p factor for each individual beam is given.

now form three bonds to the second layer iron atoms with an increased length of 2.12 Å. Despite the large relaxations all bond lengths in the surface region remain reasonable. For comparison the bond lengths in α-Fe_2O_3 are 1.96 and 2.09 Å, whereas there is only one bond length in FeO, 2.15 Å.

We have shown that well-ordered epitaxial films of iron oxide can be prepared reproducibly onto the dissimilar Pt(111) substrate. They form the Fe_3O_4 magnetite bulk structure and make it possible to study more easily the surface properties of this metal oxide with electron spectroscopy techniques. The atomic structure we find for the Fe_3O_4(111) surface clearly suggests that both the minimization of the number of dangling bonds and of the electrostatic surface energy are the driving forces for the relaxations formed on this polar metal oxide surface. This is probably due to the bond character in this oxide, which lies between a pure ionic and a pure covalent bond. This mixed character has been modeled by using empirical short range and ionic long range potentials [19] as well as by *ab initio* calculations [2], and relaxations of polar and nonpolar surfaces have been computed in the case of various alkali halides [20], α-Fe_2O_3 [2] and α-Al_2O_3 [1]. It would be very interesting to compare the predicted relaxations of such calculations for Fe_3O_4 with the relaxations obtained from this LEED study. This would help to further clarify the driving forces responsible for the surface reconstructions formed and give new insights into the interesting but still relatively unexplored problem of atomic relaxations at ionic interfaces.

W.W. gratefully acknowledges financial support from the Deutsche Forschungsgemeinschaft (DFG). We also acknowledge helpful discussions with Uli Starke and Robert Schlögl. This work was supported by the Director, Office of Energy Research, Office of Basic Energy Sciences, Materials Sciences Division of the U.S. Department of Energy under Contract No. DE-AC03-76SF-00098.

[1] I. Manassidis, A. De Vita, and M.J. Gillan, Surf. Sci. **285**, L517 (1993).

[2] W. C. Mackrodt, R. J. Davey, S. W. Black, and R. Docherty, J. Cryst. Growth **80**, 441 (1987).

[3] N. Bickel, G. Schmidt, K. Heinz, and K. Müller, Phys. Rev. Lett. **62**, 2009 (1989).

[4] M. Prutton, J. A. Ramsey, J. A. Walker, and M. R. Welton Cook, J. Phys. C **12**, 5271 (1979); R. C. Felton, M. Prutton, S. P. Tear, and M. R. Welton Cook, Surf. Sci. **88**, 474 (1979); P. Zschak in *The Structure of Surfaces III,* edited by S. Y. Tong, M. A. Van Hove, K. Takayanagi, and X. D. Xie (Springer, Heidelberg, 1991), Vol. 24; D. L. Blanchard, D. L. Lessor, J. P. LaFemina, D. R. Baer, W. K. Ford, and T. Guo, J. Vac. Sci. Technol. A **9**, 1814 (1990); M. R. Welton Cook and M. Prutton, J. Phys. C **13**, 3993 (1980); C. B. Duke, A. R. Lubinsky, B. W. Lee, and D. Mark, J. Vac. Sci. Technol. **13**, 761 (1976); G. Tarrach, D. Bürgler, T. Schaub, R. Wiesendanger, and H.-J. Güntherodt, Surf. Sci. **285**, 1 (1993).

[5] C. R. Brundle, T. J. Chuang, and K. Wandelt, Surf. Sci. **68**, 459 (1977).

[6] R. F. Faiki, A. P. Kaduwela, J. Osterwalder, D. J. Friedman, C. S. Fadley, and C. R. Brundle, Surf. Sci. **282**, 33 (1993); H. Kuhlenbeck, G. Odörfer, R. Jaeger, G. Illing, M. Mengers, Th. Mull, H. J. Freund, M. Pöhlchen, V. Staemmler, S. Witzel, C. Scharfschwerdt, K. Wennemann, T. Liedke, and M. Neumann, Phys. Rev. B **43**, 1969 (1991); O. L. Warren and P. A. Thiel (to be published).

[7] A. Ignatiev, B. W. Lee, and M. A. Van Hove, *Proceedings of the 7th International Vacuum Congress and 3rd International Conference on Solid Surfaces, Vienna, 1977,* edited by R. Dobrozemsky *et al.* (F. Berger Söhne, Vienna, 1977), p. 1.

[8] C. Zhang, M. Z. Van Hove, and G. A. Somorjai, Surf. Sci. **149**, 326 (1985).

[9] R. J. Lad and J. M. Blakely, Surf. Sci. **79**, 467 (1987).

[10] R. M. Jaeger, J. Huhlenbeck, H. J. Freund, M. Wuttig, W. Hoffmann, R. Franchy, and H. Ibach, Surf. Sci. **259**, 235 (1991).

[11] M. Barbieri, W. Weiss, M. A. Van Hove, and G. A. Somorjai (to be published).

[12] W. Weiss and G. A. Somorjai, J. Vac. Sci. Technol. A **11**, 2138 (1993).

[13] M. Muhler, R. Schlögl, and G. Ertl, J. Catal. **138**, 413 (1992).

[14] These distances can also be viewed as the hypothetical oxygen interatomic distances in the approximation of ideal hexagonal close-packed oxygen layers, which we will refer to as "ideal spinel." The real spinel structure of Fe_3O_4 (inverse spinel structure for temperatures above 115 K) consists of slightly distorted hexagonal close-packed oxygen layers, where within a (2×2) supercell one oxygen atoms moves 0.04 Å out of the plane defined by the other three oxygen atoms in that cell. R. W. G. Wyckoff, *Crystal Structures* (R. E. Krieger, Malabar, FL, 1982), 2nd ed., Vol. 2, p. 75.

[15] M. A. Van Hove and S. Y. Tong, *Surface Crystallography by LEED,* edited by R. Gomer, Springer Series in Chemical Physics 2 (Springer-Verlag, Berlin, 1979).

[16] *The Oxide Handbook,* edited by G. V. Samsonov (IFI/Plenum, New York, 1982), 2nd ed.

[17] M. A. Van Hove, W. Moritz, H. Over, P. J. Rous, A. Wander, A. Barbieri, N. Materer, U. Starke, D. Jentz, J. M. Powers, G. Held, and G. A. Somorjai, Surf. Sci. Rep. (to be published).

[18] P. J. Rous and J. B. Pendry, Comput. Phys. Commun. **54**, 137 (1989); **54**, 157 (1989); Surf. Sci. **219**, 355 (1989).

[19] C. R. A. Catlow, K. M. Diller, and M. J. Norgett, J. Phys. C **10**, 1395 (1977).

[20] P. W. Tasker, Philos. Mag. A **39**, 119 (1979).

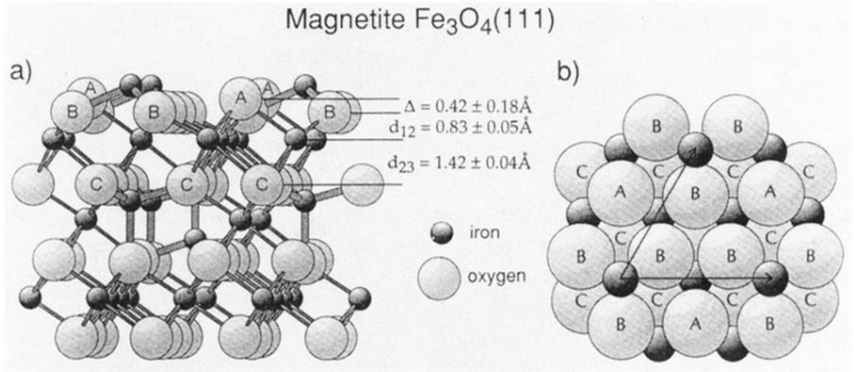

FIG. 1. (a) Perspective side view of the Fe_3O_4(111) surface structure (surface is on top). Relaxed layer spacings in the surface region are indicated. The corresponding bulk values are $\Delta = -0.04$ Å, $d_{12} = d_{23} = 1.19$ Å. Bonds formed by tetrahedral and octahedral iron atoms are drawn thick and thin, respectively. Tetrahedral sites are occupied by Fe^{3+} ions; octahedral sites are occupied randomly by 50% Fe^{2+} and 50% Fe^{3+} ions. The ionic sizes are reduced by a factor of 0.5. (b) Top view onto the Fe_3O_4(111) surface with the full ionic sizes. The lattice vectors of the (2×2) unit cell are also indicated.